



# Distinct changes in carbon, nitrogen, and phosphorus cycling in the litter layer across two contrasting forest–tundra ecotones

Frank Hagedorn<sup>1,★</sup>, Josephine Imboden<sup>1</sup>, Pavel A. Moiseev<sup>3</sup>, Decai Gao<sup>1,4</sup>, Emmanuel Frossard<sup>2</sup>, Patrick Schleggi<sup>1</sup>, Daniel Christen<sup>1</sup>, Konstantin Gavazov<sup>1</sup>, and Jasmin Fetzer<sup>1,2,★</sup>

<sup>1</sup>Forest Soils and Biogeochemistry, Swiss Federal Institute for Forest, Snow and Landscape Research WSL, Birmensdorf, Switzerland

<sup>2</sup>Dept. of Environmental Systems Science, ETH Zurich, Zurich, Switzerland

<sup>3</sup>Institute of Plant and Animal Ecology, Ural Branch, Russian Academy of Sciences, 620144, Ekaterinburg, Russia

<sup>4</sup>Qianyanzhou Ecological Research Station, The Key Laboratory of Ecosystem Network Observation and Modeling, Institute of Geographic Sciences and Natural Resources Research, Chinese Academy of Sciences, Beijing, China

★These authors contributed equally to this work.

**Correspondence:** Frank Hagedorn (frank.hagedorn@wsl.ch)

Received: 20 August 2024 – Discussion started: 10 September 2024

Revised: 23 December 2024 – Accepted: 8 January 2025 – Published: 25 June 2025

**Abstract.** At treeline, plant life forms and species change abruptly from low-stature plants in the tundra to trees in forests. Our study assesses how the vegetation shift affects the quality and elemental composition of the litter layer and consequently the microbial processing and nutrient release during decomposition. We sampled litter layers along elevation gradients across conifer- and broadleaf-dominated tree-lines in the Russian subarctic Khibiny Mountains and hemiboreal South Urals. Using microlysimeters at 5 and 15 °C, we measured carbon (C) mineralization and the release of inorganic nitrogen (N) and phosphorus (P), reflecting net N and P mineralization. Additionally, we quantified releases of dissolved organic C and N and analysed the stoichiometry and ecophysiology of microbial biomass. Our findings showed significant shifts in the chemical characteristics of the litter layer across both treeline ecotones. On average, C : N and C : P ratios decreased by 56 % and 65 %, while lignin contents increased by 110 % from tundra to forest. The consistent decrease in C : N : P ratios in the litter layer was paralleled by pronounced increases in net N and P mineralization from tundra to lower-elevation forest in both treeline ecotones. The negligible nutrient release from tundra litter was likely due to immobilization of mineralized N and P at molar C : N and C : P ratios exceeding 35 and 1100, respectively. In contrast to net nutrient mineralization, C mineralization and the release of dissolved organic C and N re-

mained largely unchanged. Microbial biomass colonizing the litter layer showed average decreases of C : N and C : P ratios by 26 % and 74 % from tundra to forest, while potential activities of C–N–P-acquiring extracellular enzymes showed no consistent pattern. Mineralization of <sup>13</sup>C-labelled glucose-6-phosphate decreased with decreasing C : N : P ratios from tundra to forest. As the <sup>13</sup>C incorporation into microbial biomass remained unaffected, substrate-use efficiency (SUE) increased along the same trajectory. Overall, our results give evidence that the vegetation shift from tundra to forest is associated with an abrupt increase in net N and P mineralization in the litter layer, accelerating nutrient cycling and increasing N and P availability. In contrast, experimental warming by 10 °C was less important for net N and P mineralization than litter composition. This indicates that indirect effects of climatic warming through changes in plant community composition with treeline advances seem to be more important for soil N and P cycling than direct temperature effects.

## 1 Introduction

Treelines represent a striking vegetation boundary with a transition from low-stature tundra plants such as graminoids and dwarf shrubs to forest trees within short distance. Globally, the position of treelines is primarily confined to growing season temperature (Körner and Paulsen, 2004; Hagedorn et al., 2020). Climate warming led to advances of tree-lines to higher altitudes in many mountainous regions over the last century, but forest expansions often lag behind climatic warming (Hagedorn et al., 2019; Büntgen et al., 2022). One of the contributing mechanisms for the retarded tree-line shift could be nutrient limitation (Sullivan et al., 2015; Gustafson et al., 2021), possibly induced by a small nutrient mineralization from nutrient-poor organic matter in tundra (Fetzer et al., 2024) at low temperatures (Parker et al., 2018; Wang et al., 2021). Nutrients bound to organic matter are released during decomposition along the continuum from litter to strongly transformed soil organic matter (SOM). In the initial phase, plant detritus is mineralized to CO<sub>2</sub> and inorganic nutrient forms or converted into microbial biomass (Berg and McClaugherty, 2020). Nutrients can subsequently be released from the residues of microbial biomass. The release of inorganic nutrients with decomposition is regarded as net nutrient mineralization (e.g. Nadelhoffer et al., 1991; Bröddlin et al., 2019). In addition, a small fraction of organic matter is also leached in organic form, transporting carbon (C) and organically bound nutrients into deeper soil horizons (Hagedorn and Machwitz, 2007; Fetzer et al., 2022). Along with climatic controls such as temperature and moisture, decomposition processes and nutrient mineralization are driven by the quality and nutrient contents of litter materials (Aerts, 1997; Gavazov, 2010; Wang et al., 2021) as well as by the soil biota colonizing decomposing litter (Zheng et al., 2018; Liu et al., 2019). In the litter layer, decomposing organisms have to degrade recalcitrant compounds, such as lignin, tannins, and melanins that are frequently interlinked with nutrient-rich and/or labile components (Adamczyk et al., 2019; Sainte-Marie et al., 2021). In addition, microbial communities face pronounced stoichiometric imbalances between their biomass and the plant residues they decompose. However, microorganisms possess various adaptation strategies to overcome nutrient limitations (e.g. Mooshammer et al., 2014; Manzoni et al., 2021). (1) To some extent, microbes can enlarge the C : nutrient ratio in their biomass, but their plasticity to adjust the biomass stoichiometry is generally considered limited due to homeostasis (Mooshammer et al., 2014). However, microbial species are found to have a wide range of element ratios (Fanin et al., 2017; Zhang and Elser, 2017; Camenzind et al., 2021). Furthermore, distinct microbial communities colonize different types of organic material (Kaiser et al., 2015; Solly et al., 2017a; Zheng et al., 2018). (2) Another strategy is the production of extracellular enzymes, which is coupled to the uptake of C and nutrients and the adjustment of nutrient

turnover in microbial biomass (Spohn and Widdig, 2017). (3) Microorganisms can also regulate their element use efficiency by releasing nutrients or carbon exceeding their demand (Mooshammer et al., 2014). (4) Additionally, fungi translocate nutrients from the soil into the nutrient-poor litter layer via their hyphae to alleviate nutrient imbalances (Spohn and Berg, 2023). When nutrients are scarce, microorganisms lack the nutrients needed to produce microbial biomass, which results in a low carbon-use efficiency (CUE) with high respiratory C losses relative to biomass production (Manzoni et al., 2021). Mineralized nutrients are then immobilized or recycled in microorganisms (Siegenthaler et al., 2024). The switch from C or energy limitation to nutrient limitation is observed to occur at distinct threshold element ratios (TERs), which are well established for C : N ratios (of around 20 on a molar basis; Mooshammer et al., 2014). However, empirical TERs are less certain for C : P, with reported molar ratios in forest litter ranging widely from 300 to 1700 (Moore et al., 2011). These values also vary depending on the type of organic material (Heuck and Spohn, 2016).

Since litter decomposition is largely controlled by plant species and local abiotic conditions (Gavazov, 2010; Joly et al., 2023), the abrupt change in plant species and environmental conditions across treelines impacts litter decomposition and consequently nutrient release. In situ litterbag studies using standardized plant leaf litter in the sub-Arctic Scandes, the Tibetan Plateau, and the Urals provide evidence of slower litter decomposition in tundra ecosystems compared to forests below treeline (Liu et al., 2016; Solly et al., 2017b; Parker et al., 2018; Wang et al., 2021). This difference is attributed to the lower quality of tundra litter, characterized by high contents of recalcitrant compounds and elevated C : N : P ratios (Zheng et al., 2018) as well as the less favourable microclimate in tundra than under forest canopies (Kammer et al., 2009; Parker et al., 2018). Substantially less is known on the release of nutrients from decomposing litter of the treeline ecotone. Generally, tundra plants growing in nutrient-poor soils produce nutrient-poorer litter than in forests (Wang et al., 2021; Fetzer et al., 2024). In conjunction with the observed slower litter mass loss, this strongly suggests that nutrient release from decomposing litter will be smaller in tundra than in forests. This might contribute to the decline in nutrient availability from forests towards tundra (Mayor et al., 2017; Fetzer et al., 2024), which in turn could reduce tree growth and forest expansion (Kammer et al., 2009; Hagedorn et al., 2019).

Our study aimed (1) to provide a comprehensive assessment of how C, N and P release in organic or inorganic forms during litter decomposition varies across forest–tundra ecotones and (2) to examine how microorganisms cope with changes in stoichiometry and organic constituents in the litter layer along the transition from forest towards tundra. We sampled litter layers along elevation gradients ranging from the boreal forests to the tree-free tundra in the South Urals and Khibiny Mountains (Kola Peninsula). Here, treelines re-

mained largely untouched from anthropogenic land use and have advanced by 4 to 8 m in elevation per decade due to climatic changes (Hagedorn et al., 2014; Moiseev et al., 2022). As the dominant treeline species is coniferous (*Picea obovata*) in the metamorphic South Urals and deciduous (*Betula pubescens*) in the plutonic Khibiny Mountains, we assumed that sampled litter layers encompassed a strong gradient of organic compounds and stoichiometry. In the laboratory, we conducted a 12-week-long microcosm study to measure potential C mineralization and the release of inorganic and organic N and P at 5 and 15 °C. In addition, we studied the responses of microbial ecophysiology to the range of litter layer characteristics across the two treelines by (i) analysing C : N : P ratios in microbial biomass; (ii) measuring the activity of extracellular enzymes hydrolyzing organic C, N, and P compounds; and (iii) determining the metabolic quotient ( $q\text{CO}_2$ ) as well as the use of labile  $^{13}\text{C}$ -labelled glucose-6-phosphate (G6P) by microorganisms, and (iv) quantifying net P mobilization or immobilization from the added G6P.

(1) We hypothesized that the potential release of C, N, and P from the litter layer would increase from tundra to forest due to an improved litter quality reflected by decreasing C : N : P ratios and an altered composition in organic constituents. We expected that the increase in net N and P mineralization would be greater than that of C, as microorganisms in tundra are more likely to immobilize released N and P due to the higher C : N : P ratios in tundra litter compared to forest litter. (2) We anticipated that microbial ecophysiology would adapt to the decreasing litter stoichiometry from tundra to forest by reducing extracellular enzyme production and enhancing substrate-use efficiency (SUE), with lower  $\text{CO}_2$  respiration per unit biomass in the nutrient-rich forest litter layer. However, we expected that changes in the C : N : P ratio of microbial biomass would remain small due to the homeostatic nature of microbial biomass. (3) We concluded that increasing temperature would enhance the release of inorganic and organic C, N, and P but to a different extent.

## 2 Material and methods

### 2.1 Study sites and sampling

Releases of C, N, and P as well as microbial functioning were studied in the litter layer of forest–tundra ecotones in two Eurasian mountain ranges, the Khibiny Mountains on the Kola Peninsula (67° N, 34° E) and on the Iremel Massif in the South Urals (54° N, 58° E) denoted hereafter as South Urals (S Urals) (Fig. S1 in the Supplement). In both regions, litter layers were collected during the peak growing season (July) along two replicate elevation transects crossing the treeline ecotone reaching from the treeless tundra to the forest. They covered approx. 150 m in elevation, ranging from 325 to 470 m a.s.l. in the Khibiny Mountains and from 1260 to 1405 m a.s.l. in the S Urals. The transects in

both mountain ranges were located on gentle slopes of less than 10°. While the parent material in the Khibiny Mountains is plutonic rock that is rich in apatite, it is chlorite–illite–quartz shales in the S Urals. Soil types are podzolised sandy Rankers in Khibiny and loamy Cambisols in the S Urals with pH values of 4.1 and 3.5 at 0–10 cm depth in Khibiny and S Urals, respectively. The dominant tree species is a conifer, Siberian spruce (*Picea obovata* Ledeb.), in the S Urals, while in Khibiny a broadleaf species *Betula pubescens* ssp. *tortuosa*, Czerepanovii, dominates. The ground vegetation of the tundra in both regions is dominated by dwarf shrubs such as *Vaccinium* species, *Empetrum*, *Betula nana*, mosses, and lichens (Fig. S1). In the S Urals, there are also grasses and sedges such as *Carex vaginata* Tausch and *Festuca igoschiniae* Tzvelev (Solly et al., 2017b). The forest at lower elevation consists also of open areas without tree canopy, which is dominated by up to 2 m tall herbs (*Polygonum bistorta* L., *Polygonum alpinum* All.) in the S Urals (Solly et al., 2017b), while in Khibiny a mix of ferns, mosses, and herbaceous plants along with dwarf shrubs (*Vaccinium* spp.) and *Empetrum* prevails. In both regions, the litter layer was sampled at three elevation levels across the forest–tundra ecotone: (i) “tundra” without trees where shrubs, herbs, lichens, and mosses dominate; (ii) “treeline” with the uppermost trees (>2 m, 4 m on average) growing in clusters (tree crown cover < 10 %), and (iii) the “forest” at lowest elevation with approx. 10 m tall trees and a tree crown cover of 38 % (Solly et al., 2017b). Within these elevation levels, the litter layer was sampled in randomly selected plots (1 m × 1 m) under the tree “canopy” that is typical for the respective elevation level in terms of age class and height and an adjacent subplot (1 m × 1 m) in the “open land”, a canopy-free area with shrubs and herbaceous plants in between tree clusters (distance to trunk 2.5–6 m) (Solly et al., 2017b). Each of these ecosystem types was sampled in three randomly selected plots that were distributed along horizontal distances of 2 km in Khibiny and 5 km in the S Urals. Overall, our sample set comprised five ecosystem types, replicated across two elevation transects in each of the two mountain regions: (1) tundra, (2) treeline–canopy, (3) treeline–open land with tundra-type vegetation, (4) forest–canopy, and (5) forest–open land between forest patches. Samples were stored at 4 °C until incubation in the laboratory.

### 2.2 Litter C–N–P release experiment

Microcosms were used to simultaneously quantify potential C mineralization, net N and P mineralization, and DOC and DON release. Material from the litter layer (10 g of fresh sample cut into 2 cm × 1 cm pieces) was placed in filtration systems (Millipore Stericup, 250 and 500 mL) that were leached repeatedly to measure element release in the leachate (Bröddlin et al., 2019). To prevent clogging of the 0.45 µm Durapore membrane filters of the microlysimeters, a glass fibre filter (GF 6 100, Hahnemühle FineArt GmbH, DE, 80 g,

0.35 mm, inorganic binder) was put on top of the filters. In addition, we wrapped the samples into nylon net filters (approx. 2  $\mu\text{m}$ ) which were tied up with a polyamide cord (1.3 mm) to avoid floating of litter material and to allow the replacement of microlysimeters when filters were clogged.

Following an initial leaching to standardize moisture conditions and remove nutrients released upon sample storage and processing, litter layer samples were incubated for 2 weeks in a climate chamber at 15 °C and leached on a weekly basis to precondition the litter samples (Canali and Benedetti, 2006). Afterwards half the samples were transferred to a climate chamber at 5 °C, while the remaining stayed at 15 °C to cover the soil temperature range during the growing season. Another 2 weeks later, we started the experiment, measuring the C, N, and P release repeatedly after 1, 2, 3, 4, 6, 8, and 12 weeks. The experiment comprised 60 litter microcosms (2 regions  $\times$  5 ecosystem types  $\times$  3 plots  $\times$  2 temperatures). Four additional samples without litter material served as controls, with two of them incubated in each climate chamber. Carbon mineralization was determined for the entire week in between leaching cycles by placing the microlysimeters into airtight containers (1000 mL) and trapping respired  $\text{CO}_2$  in 25 mL of 0.05 to 0.1 M NaOH. The amount of  $\text{CO}_2$  trapped was determined by immediately measuring the reduction in electrical conductivity calibrated by titration with HCl following  $\text{BaCl}_2$  addition. The molarity of NaOH was adjusted during the course of the experiment.

For the leaching, 100 mL of nutrient solution similar to the nutrient solution found in organic layers ( $400 \mu\text{mol L}^{-1}$   $\text{CaCl}_2$ ,  $50 \mu\text{mol L}^{-1}$   $\text{K}_2\text{SO}_4$ , and  $50 \mu\text{mol L}^{-1}$   $\text{MgSO}_4$ ; Brödlén et al., 2019) was added to the microlysimeters. A glass disc was placed on top of litter samples to avoid floating of litter materials and to ensure homogenous wetting. After 1 h, the microlysimeters were leached using a vacuum pump (EcoTech, Bonn, Germany) with a suction of 200 hPa. The volume of the leachate was determined gravimetrically.

### 2.3 Chemical analyses of leachates

In the leachates, we measured DOC and total dissolved nitrogen (TDN) with a TOC/TN analyser (TOC-L, Shimadzu, Corp. Tokyo, Japan).  $\text{NH}_4^+$  concentrations in leachates were analysed colourimetrically using a flow injection system FIAS-400 and a UV-VIS spectrometer Lambda 2S (PerkinElmer, Waltham, MA, United States). Ion chromatography was used to determine  $\text{NO}_3^-$  concentrations (ICS 3000, Dionex, Sunnyvale, CA, United States). Phosphate concentrations were measured with the malachite green method (Ohno and Zibilske, 1991). Total dissolved P was determined as  $\text{PO}_4^{3-}$  with the malachite green method after the extract was oxidized with ammonium persulfate dissolved in 0.9 M  $\text{H}_2\text{SO}_4$  and autoclaved (Tiessen and Moir, 1993). Dissolved organic N and DOP concentrations were calculated by sub-

tracting dissolved inorganic N or P from TN or TP, respectively.

### 2.4 Chemical analyses of litter layer

Litter layer C and N contents were analysed by an Elemental analyser (EuroVector EA3000, Pavia, Italy). For P, K, Ca, Mg, and Mn in ground litter, samples were first digested in 8 M  $\text{HNO}_3$  with 0.6 M HF in a microwave digestion unit (MW ultraCLAV, MLS, Milestone Inc., Shelton, CT, USA). Then, total element concentrations were measured using ICP-OES (Optima 7300 DV, PerkinElmer, Waltham, MA, USA). Lignin contents were determined by extracting 1 g of ground sample three times with 25 mL of hot water and once with cold water (extraction time 15 min each). The residues of the hot-water-extracted samples were first extracted four times with 25 mL of ethanol. An aliquot was then hydrolyzed with 72 % sulfuric acid and autoclaved. In the extract, the amount of acid soluble lignin (ASL) was measured with a photometer at 205 nm, while the contents of Klason lignin were determined gravimetrically after incineration of remaining litter materials at 550 °C for 4 h.

Additionally, a subsample of ground litter was analysed by Fourier transform infrared spectroscopy (FT-IR) using a Vertex70 FT-IR spectrometer with high-throughput screening extensions by Bruker Optics (Massachusetts, USA) to identify major functional groups in litter (Kammer et al., 2009). The following bands were evaluated (Duboc et al., 2012):  $2920 \text{ cm}^{-1}$  representing aliphatic C–H stretches,  $1650 \text{ cm}^{-1}$  representing C=O of carboxylates and aromatic C=C vibration,  $1515 \text{ cm}^{-1}$  representing C=C of aromatic groups, and  $1270$  and  $1230 \text{ cm}^{-1}$  representing benzoic acids and C–O of (aryl) esters and of phenolic groups (Tatzber et al., 2010; Duboc et al., 2012).

### 2.5 Microbial biomass C, N, P, and enzyme activities

After the 12-week-long incubation, microbial biomass C, N, and P in litter layers were estimated by the chloroform fumigation–extraction method (Brookes et al., 1982; Brookes et al., 1985; Vance et al., 1987). Briefly, litter was split into two aliquots, equivalent to 0.75 g dry mass. One aliquot was fumigated with chloroform at 25 °C for 24 h. Fumigated and non-fumigated litter subsamples were extracted with 15 mL of 0.05 M  $\text{K}_2\text{SO}_4$  after shaking them for 1 h with 200 rpm (Brookes et al., 1985; Makarov et al., 2015). Organic C and total N concentrations in the extracts were then determined with a Shimadzu TOC/TN analyser (TOC-V, Shimadzu, Tokyo, Japan). Microbial biomass C and N were calculated from the difference in extracted C and N between fumigated and non-fumigated litter, divided by the extraction efficiency coefficient  $k_{\text{EC}} = 0.45$  (Vance et al., 1987) and  $k_{\text{EN}} = 0.54$  (Brookes et al., 1985), respectively. For microbial biomass P, fumigated and non-fumigated litter subsamples were extracted with 0.5 M  $\text{NaHCO}_3$  (pH = 8.5) af-

ter shaking them for 1 h with 200 rpm (Brookes et al., 1982). Then, inorganic P in the extracts was determined using the malachite green method. To correct the P fixation during the  $\text{NaHCO}_3$  extraction, a spike of  $\text{KH}_2\text{PO}_4$  equivalent to  $25 \mu\text{g P g}^{-1}$  soil was used. Finally, microbial biomass P was calculated from the difference of the two extracts divided by  $k_{\text{EP}} = 0.45$  (Brookes et al., 1982; Wu et al., 1990).

The potential activities of five extracellular enzymes in the litter layer were determined using fluorogenic substrates according to the method described by Saiya-Cork et al. (2002). The enzymes and substrates were  $\beta$ -glucosidase (EC 3.2.1.21) and  $\beta$ -xylosidase (EC 3.2.1.37) assayed with 4-methylumbelliferyl (MUB)- $\beta$ -D-glucosidase and MUB- $\beta$ -D-xylopyranoside, respectively, involved in C cycling; N-acetylglucosaminidase (EC 3.2.1.30) and leucine aminopeptidase (EC 3.4.11.1) assayed with MUB-N-acetyl- $\beta$ -D-glucosaminide and L-leucine-7-amido-4-methylcoumarin hydrochloride (L-leucine-AMC), respectively, involved in N cycling; and monoester phosphatases (EC 3.1.3.2) assayed with MUB phosphate, involved in P cycling. Before assaying soil enzyme activity, the concentration of fluorogenic substrates was optimized to ensure saturated substrate concentrations (German et al., 2011). Briefly, 0.5 g (dw, dry weight equivalent) of moist litter samples was mixed with 100 mL sodium acetate buffer (pH = 5.0) and stirred on a magnetic plate for 1 min. 200  $\mu\text{L}$  litter suspensions and 50  $\mu\text{L}$  specific substrates, fluorescently labelled with AMC or MUB, were added to assay 96-well microplates. The AMC- and MUB-linked substrates were used to measure leucine-amino-peptidase and all other hydrolytic enzymes, respectively. 200  $\mu\text{L}$  litter suspensions, 50  $\mu\text{L}$  buffer and 200  $\mu\text{L}$  buffer, and 50  $\mu\text{L}$  MUB or AMC were added into quench and standard 96-well microplates, respectively. All microplates were incubated in the dark at 25 °C for 4 h, and then 10  $\mu\text{L}$  of 0.5  $\text{mol L}^{-1}$  NaOH was added to terminate the assay. Fluorescence was measured using a microplate reader (Synergy H1, BioTek, Winooski, VT, USA) at 365 nm excitation and 450 nm emission. The potential activities of litter extracellular enzymes were presented in units of  $\text{nmol g}^{-1}$  dry soil  $\text{h}^{-1}$  and calculated according to German et al. (2011) (see formula in Supplement S2).

## 2.6 Substrate-use efficiency by tracking $^{13}\text{C}$ -glucose-6-phosphate

Following the 12-week-long incubation, we quantified the mineralization of  $^{13}\text{C}$  labelled G6P ( $^{13}\text{C}_6\text{H}_{11}\text{O}_9\text{PNa}_2 \times (\text{H}_2\text{O})_x$ , by Omicron Biochemicals.) to determine substrate-use efficiency (SUE). In the experiment, litter layer material from both temperature incubations (2.4 g dry weight equivalent) was transferred in 150 mL glass jars (Schott), and then 3 mL of a  $^{13}\text{C}$ -labelled G6P solute containing 6.76 mg  $^{13}\text{C}$  was added to each sample, which corresponded to 0.64 % of C and  $5 \pm 0.6$  % of P in the litter sample. Control samples received the same

amount of solute as water. For each measurement of  $^{13}\text{C}$  mineralization, the container with the samples was first flushed with  $\text{CO}_2$ -free air. Then, the jars were closed with a septum and gas samples of the headspace were taken after a set incubation period (see below) with a 15 mL syringe and injected into pre-evacuated glass vials (12 mL volume, Exetainer gas testing vials; Labco, High Wycombe, UK). Samples were incubated for 4 h and 1 h at 5 and 15 °C, respectively. The  $\delta^{13}\text{C}$  values of respired  $\text{CO}_2$  were measured by connecting the pressurized vials to a GasBench II (Delta PlusXL; Thermo Finnigan).  $^{13}\text{C}$  mineralization was determined immediately, 4, 24, 48, 72, and 168 h after adding  $^{13}\text{C}$ -labelled G6P. Regular weight measurements ensured a constant water content during the experiment. An aliquot of the litter sample was then extracted with 0.05 M  $\text{K}_2\text{SO}_4$  either before or after fumigation with chloroform. In these extracts, the  $^{13}\text{C}$  was oxidized to  $\text{CO}_2$  using  $\text{K}_2\text{S}_2\text{O}_8$  that was measured as  $^{13}\text{CO}_2$  as described above.

## 2.7 Data analysis and statistics

Net C, N, and P release was estimated by multiplying C, N, and P concentrations with the volume of the leachate. When concentrations were below the detection limit, half this value had been used for the calculation. For the longer time periods towards the end of the experiment, we interpolated linearly between two measurements. The temperature dependencies of C, N, and P release were evaluated by calculating  $Q_{10}$  values in the following equation:

$$Q_{10} = (k_2/k_1)^{10/(T_2-T_1)}, \quad (1)$$

where  $k_1$  is the measured process rate (e.g. C mineralization) at temperature  $T_1$ , here 5 °C, and  $k_2$  is the process rate at temperature  $T_2$ , here 15 °C.  $Q_{10}$  values could not be calculated for N and P release from tundra litter where element concentrations in leachates remained below detection limits.

The metabolic quotient  $q\text{CO}_2$  was calculated as the ratio of respired C and microbial C in the 12th week at the end of the incubation experiment. Microbial SUE was estimated as

$$\text{SUE} = {}^{13}\text{C}_{\text{microbial}} / ({}^{13}\text{C}_{\text{microbial}} + {}^{13}\text{CO}_2), \quad (2)$$

where  $^{13}\text{C}_{\text{microbial}}$  is the  $^{13}\text{C}_{\text{excess}}$  in microbial biomass measured by CFE (e.g. Gao et al., 2021) and  $^{13}\text{CO}_2$  the amount of respired  $\text{CO}_2$  from the added G6P.

The net recovery of P in leached dissolved inorganic P (DIP) as compared to the amount of P added by G6P was calculated from a simple mass balance as

$$\text{net DIP recovery} = (\text{DIP}_{t1} - \text{DIP}_{t0}) / \text{G6P}_{\text{added}}, \quad (3)$$

with  $\text{DIP}_{t1}$  and  $\text{DIP}_{t0}$  being the amount DIP leached after and before the addition of G6P.

Data were statistically analysed by fitting linear mixed effect models by the restricted maximum likelihood (lme function of the nlme package; Pinheiro et al., 2021; R version

**Table 1.** Selected chemical properties of the litter for the five ecosystem types (tundra, open- and closed-forest patches at the treeline, and open- and closed-forest patches in the established forest) along the elevational gradients at Khibiny and the South Urals (S Urals). Values given for tannins, aliphatic components, and aromaticity are relative measures derived from FT-IR spectra (Duboc et al., 2012; Fig. S1). Statistical significance ( $P$  values) was tested with a linear mixed-effects model (LME). Numbers in bold stand for statistically significant results ( $p < 0.05$ ).

Region	Elevation	Vegetation	C <sub>tot</sub> (g kg <sup>-1</sup> )	N <sub>tot</sub> (g kg <sup>-1</sup> )	P <sub>tot</sub> (mg kg <sup>-1</sup> )	Klason lignin (g kg <sup>-1</sup> )	Tannins 1620 (cm <sup>-1</sup> )	Aliphatic 2920 (cm <sup>-1</sup> )	Aromaticity index
Khibiny	Tundra	Open	442	11.1	1052	388	1.62	1.40	1.00
		Treeline	448	11.4	1054	434	1.66	1.39	0.97
	Tree	Open	476	18.1	1302	533	1.70	1.33	0.88
		Forest	454	14.7	1588	469	1.62	1.31	0.93
	Tree	Open	454	22.1	1975	553	1.73	1.28	0.84
		Forest	454	22.1	1975	553	1.73	1.28	0.84
S Urals	Tundra	Open	411	8.0	384	131	1.45	1.43	1.13
		Treeline	415	8.6	498	171	1.43	1.39	1.10
	Tree	Open	427	19.1	1261	416	1.62	1.33	0.90
		Forest	439	14.5	835	374	1.51	1.26	0.88
	Tree	Open	451	21.3	1481	528	1.69	1.35	0.85
		Forest	451	21.3	1481	528	1.69	1.35	0.85
Significance									
Region			< 0.001	NS	< 0.001	< 0.001	< 0.001	NS	0.045
Elevation			0.004	< 0.001	< 0.001	< 0.001	< 0.001	< 0.001	< 0.001
Vegetation			0.02	< 0.001	< 0.001	< 0.001	< 0.001	NS	< 0.001
Region × elevation			0.02	NS	0.06	< 0.001	0.02	NS	0.022
Region × vegetation			NS	NS	0.006	0.008	< 0.001	NS	NS
Elevation × vegetation			0.02	NS	NS	0.045	NS	0.02	0.14

NS: non-significant.

3.6.2, R CoreTeam, 2020). The model included the fixed effects region, elevation distance relative to the treeline, vegetation type (canopy or open land), and temperature as well as their two-way interactions, while microcosm was the random effect. The corAR1 function was included in the model to account for repeated measurements per microcosm. Elevation distance relative to the treeline was used as a numerical variable to indicate the direction and position relative to the treeline with the tundra being 50 m above treeline and the forest being 100 m below treeline. Response variables were log-transformed before the analysis. Residuals of the models were tested for normal distribution using a Shapiro–Wilk normality test.

### 3 Results

#### 3.1 Litter layer characteristics

The litter layer showed distinct chemical composition across the treeline ecotones in both regions. Total N and P contents strongly increased with decreasing elevations from the tundra to the forest (Table 1;  $p_{\text{elevation}} < 0.001$ ). For instance, P contents were 3.0 and 1.7 times greater in the forest than

in the tundra in the Khibiny Mountains and S Urals, respectively. They were also greater under tree canopies than under open vegetation areas in the tundra and in between tree clusters (Table 1;  $p_{\text{vegetation}} < 0.001$ ). The litter layer of the two regions showed similar N contents ( $p_{\text{region}} = \text{n.s.}$ ), while P contents were about 60 % greater in the Khibiny Mountains with a plutonic bedrock than in the S Urals with a quartzitic bedrock ( $p_{\text{region}} < 0.001$ ; Table 1). These differences between mountain regions were particularly pronounced in the litter layer in the open areas. Element ratios showed analogous patterns. Molar C : N ratios of litter layer decreased from 63 in the tundra to 24 in the forest under tree canopy and 37 in the open areas ( $p_{\text{elevation}} < 0.001$ ). C : P ratios showed even stronger declines from the tundra to the forest than C : N ratios. Contents of Ca, Mg, and Mn in the litter layer increased from tundra towards forest ( $p_{\text{elevation}} < 0.001$ ), while K and Fe showed no consistent pattern (Table S1 in the Supplement).

Klason lignin contents increased from tundra to the forest (Table 1), ranging between 13 % in the tundra and 55 % under tree canopy in the forest of S Urals ( $p_{\text{elevation}}$  and  $p_{\text{vegetation}} < 0.001$ ). The differences were more pronounced in the S Urals with litter from conifer trees in

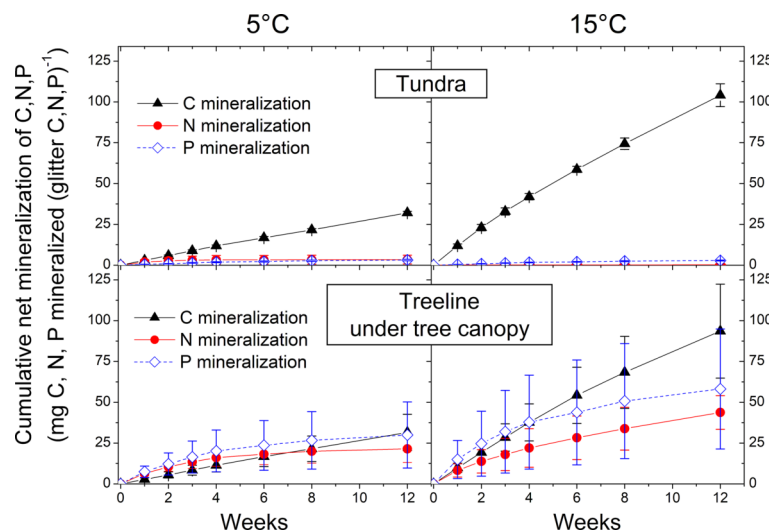


**Figure 1.** Cumulative potential net C, N, and P mineralization from the litter layer of the treeline ecotone in the South Urals at 5 and 15 °C during 12 weeks following a 3-week-long preincubation at 15 °C. Means and standard errors of three replicates. Cumulative values after 12 weeks of all vegetation types along the elevation gradient in the Khibiny Mountains and South Urals are shown in Fig. 2.

the forest than in the Khibiny Mountains with broadleaf trees ( $p_{\text{region} \times \text{vegetation}} < 0.01$ ). Measured lignin contents correlated closely with the absorbance of FT-IR spectra at wavelength of  $1515 \text{ cm}^{-1}$  ( $R^2 = 0.83^{***}$ ) and the aromaticity index ( $R^2 = 0.81^{***}$ ) (Fig. S1). These spectra indicated the greatest share of aromatic C=C in litter in the forest ( $p_{\text{elevation}} < 0.001$ ) and under canopies ( $p_{\text{vegetation}} < 0.001$ ; Table 1). Absorbance at  $1620 \text{ cm}^{-1}$  as an indicator for the abundance of C–O of carboxylates and aromatic C=C related to tannins suggests a high share of these compounds under trees ( $p_{\text{vegetation}} < 0.001$ , Fig. S2 in the Supplement, Table 1). In contrast, absorbance at  $2920 \text{ cm}^{-1}$  as a relative measure for aliphatic C–H stretches was greatest under tundra vegetation and decreased significantly from tundra to the forest level ( $p_{\text{elevation}} < 0.001$ , Table 1; Fig. S2).

### 3.2 Carbon, nitrogen, and phosphorus release

During the 12-week-long incubation experiment, total C loss by mineralization and leaching at 15 °C averaged 8.6 % of the initial C stock in the litter layer (Figs. 1, 2, and S3 in the Supplement). Carbon mineralization was the primary pathway of C-loss, accounting for 92 % of the C loss from the litter layer. Less than 1 % of the C stock in the litter layer was leached as DOC (Fig. 2). The contribution of DOC leaching to total C loss from the litter layer varied, ranging from 7 % under tundra vegetation to 20 % under coniferous trees in the S Urals ( $p_{\text{vegetation}} < 0.01$ ; Fig. 2). Carbon mineralization was greater in the S Urals than in the Khibiny Mountains ( $p_{\text{region}} < 0.001$ ). Also, the effect of vegetation type depended upon the region (Table 2). While C mineralization was smaller in the litter layer under canopies of spruce trees than under open areas in the S Urals, there was no difference

between these vegetation types in the Khibiny Mountains dominated by birch ( $p_{\text{region} \times \text{vegetation}} < 0.001$ ). Nevertheless, the difference in litter C mineralization between the two vegetation types was modest with on average 16 % higher rates in the tundra than in the forest ( $p_{\text{vegetation}} < 0.001$ ; Figs. 1 and 2). Carbon mineralization correlated negatively and most closely with lignin contents ( $R^2 = 0.55^{***}$ ) and showed a weakly positive correlation with C : N ratios ( $R^2 = 0.15^*$ ) and C : P ratios ( $R^2 = 0.30^{***}$ ) of the litter layer (Fig. 3). No correlation existed between C mineralization and contents of Ca, K, Mg, and Mn in the litter layer.

The release of inorganic N and P from the litter layer representing potential net N and P mineralization was substantially smaller than C mineralization when related to their element contents (Figs. 1 and 2). In both regions, net N mineralization rates remained close to the detection limit in the tundra and significantly increased at and beneath the tree-line ( $p_{\text{elevation}} < 0.001$ ; Table 2). It also differed strongly between vegetation types ( $p_{\text{vegetation}} < 0.001$ ; Fig. 2). In open areas, net N mineralization from the litter layer was negligible ( $< 0.2$  % of its N content), while substantial amounts of N were mineralized from tree canopy litter, reaching up to 6 % of the N contents being mineralized in 12 weeks at 15 °C at the lowest elevation. Overall, net N mineralization exhibited threshold-type relation with C : N ratios of litter materials (Fig. 4); net N mineralization from litter ceased above C : N ratios of 35 (on a molar basis). Tundra litter had C : N ratios above this threshold element ratio, while tree canopy litter was below it.

The DON release correlated closely with DOC release among litter types (for cumulative releases:  $R^2 = 0.77^{***}$ ; Fig. 3). The molar DOC : DON ratio of released DOM ranged between 23.5 under tree canopy and 168 in the tundra



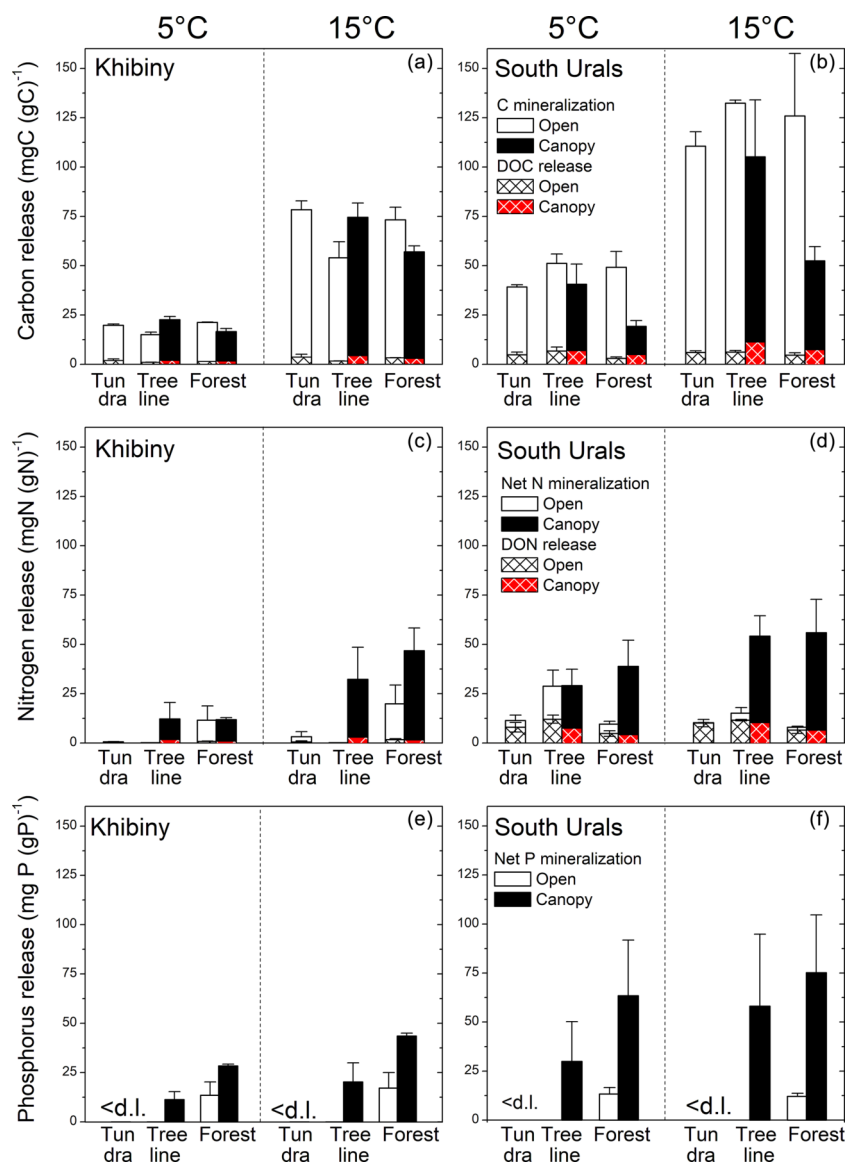


**Figure 2.** Cumulative net mineralization of carbon, nitrogen, phosphorus, and the release of organic carbon and nitrogen (DOC and DON) from the litter layer along elevation gradients across the treeline ecotone in the Khibiny Mountains (a, c, e) and South Urals (b, d, f) at 5 and 15 °C during 12 weeks of incubation. Means and standard errors of three replicates. Open land consists of areas without tree canopy, with tundra vegetation in the tundra and at treeline, and forbs in the forest.

( $p_{\text{elevation}} < 0.001$ ; data not shown). Amounts of DON released from the litter layer were greater under the tree canopy than in the open areas ( $p_{\text{vegetation}} = 0.035$ ). However, due to the negligible net N mineralization from tundra litter and hence release of inorganic N, the contribution of DON to the total N release was greater in the tundra (60 %) as compared to the tree canopy (13 %) ( $p_{\text{vegetation}} < 0.001$ ).

Overall, potential net P mineralization correlated significantly with potential net N mineralization across litter types ( $R^2 = 0.70^{***}$ ; Fig. 3). On average, net P mineralization was 20 % higher than N mineralization when normalized to element contents (Figs. 1 and 2). In the litter layer under tun-

dra vegetation, concentrations of P in leachates from tundra litter remained consistently below the detection limit of  $0.3 \text{ mg PL}^{-1}$ , and thus, net P mineralization was negligible. Concentrations of DOP were also mostly below detection limits in all litter layers. Net P mineralization strongly increased towards the forest (Fig. 2). The greatest net P mineralization occurred in the litter layer under tree canopy in the forest reaching up to 8 % of its P contents being mineralized during 12 weeks at 15 °C ( $p_{\text{elevation}}$  and  $p_{\text{vegetation}} < 0.001$ ). The threshold for net P mineralization was at a molar C : P ratio of approximately 1100 (Fig. 4). Tundra litter had higher C : P ratios, and thus net mineralization was negligible, while



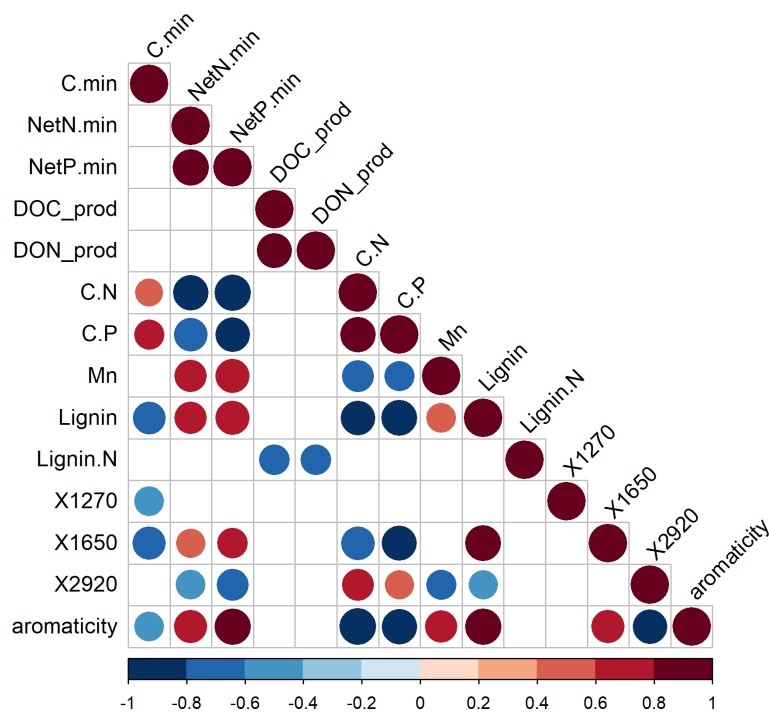


**Figure 3.** Spearman rank correlation coefficients among C mineralization, net N mineralization, net P mineralization, release of dissolved organic C (DOC), dissolved organic nitrogen (DON) during 12 weeks, and measures of the chemical quality of the litter layer across the forest–tundra ecotone in the two mountain ranges. The terms “min” and “prod” refer to mineralization and production/release; C.N and C.P are molar litter C : nutrient ratios; manganese (Mn), lignin, and nitrogen in lignin (Lignin.N) are litter composition parameters. X1270, X1650, and X2920 are values of the FT-IR spectrum at given wavelengths that are proxies for phenolic groups, aromatic compounds, and aliphatic stretches, respectively.

**Table 2.** Statistical significance (*p* values) of the linear mixed-effects model (LME) testing the effects of region, elevation, vegetation, incubation temperature, and their interaction on cumulative net C–N–P mineralization, as well as DOC and DON release during 12 weeks. Numbers in bold stand for statistically significant results (*p* < 0.05).

	C mineralization	DOC release	DON release	Net N mineralization	Net P mineralization
Region	< 0.001	< 0.001	< 0.001	< 0.01	0.05
Elevation	0.01	NS	NS	< 0.001	< 0.001
Vegetation	< 0.001	< 0.01	0.035	< 0.001	< 0.001
Temperature	< 0.001	< 0.001	0.09	NS	NS
Region × elevation	0.07	NS	0.001	0.04	NS
Region × vegetation	< 0.001	NS	0.01	NS	0.01
Elevation × vegetation	< 0.001	NS	0.04	NS	S

NS: non-significant.

tree canopy litter in the forest had lower C : P ratios and showed substantial net P mineralization.

### 3.3 Microbial biomass and extracellular enzyme activity

Microbial biomass in the litter layer was similar for the two regions but showed smaller pool sizes under tree canopies than in open vegetation (*p*<sub>vegetation</sub> < 0.001; Table 3). Ra-

tios of C : N and C : P in microbial biomass were higher in Khibiny than in the S Urals (Fig. 5). In each region, they correlated significantly with the ratios in the litter layer (Fig. 5) and decreased from the tundra litter with high C : N : P ratios to the forest with lower ratios. Microbial N : P ratios showed the same decline towards lower elevations as those of the litter layer (*p*<sub>elevation</sub> < 0.001; Table 3). Molar N : P ratios in microbial biomass reached from 5 in the litter layer of the forest up to 20 in tundra (Fig. 5). The

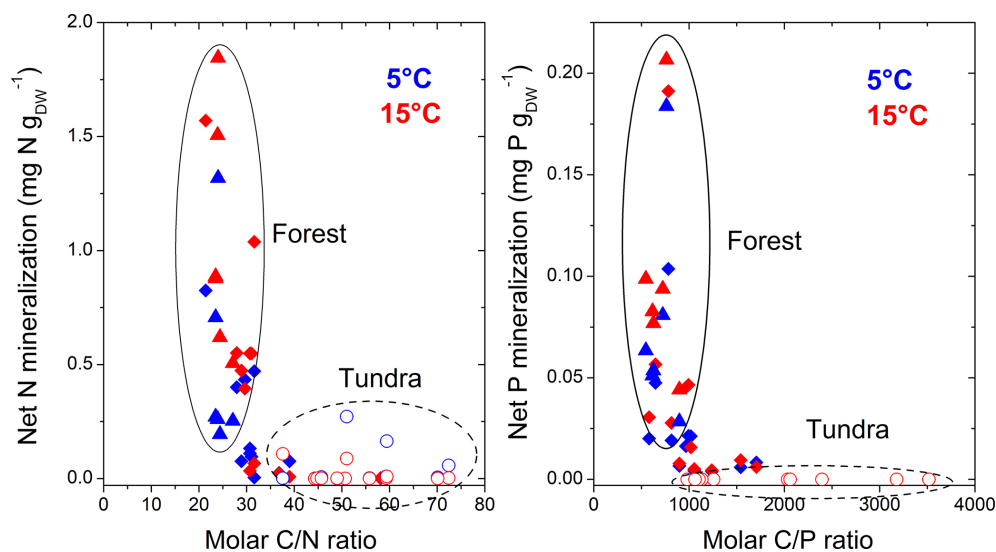


**Figure 4.** Relationship between the molar C : N and C : P ratios of litter materials, and cumulative net N and P mineralization, during 12 weeks at 5 and 15 °C in the Khibiny Mountains and S Urals. Open circles represent rates from tundra litter, closed triangles represent those from tree canopy litter in the forest, and rhomboids represent those at treeline in the two mountain regions.

**Table 3.** Statistical significance (*p* values) of the linear mixed-effects model (LME) testing the effects of region, elevation, vegetation, incubation temperature, and their two-way interactions on microbial biomass and carbon (MB-C), their C : N and C : P ratios, and the metabolic quotient (*q*CO<sub>2</sub>) and substrate-use efficiency (SUE). Numbers in bold stand for statistically significant results (*p* < 0.05).

	MB-C	MB-C : N	MB-C : P	MB-N : P	<i>q</i> CO <sub>2</sub>	SUE
Region	0.05	<b>&lt; 0.001</b>	<b>&lt; 0.001</b>	<b>&lt; 0.001</b>	<b>&lt; 0.001</b>	<b>&lt; 0.001</b>
Elevation	NS	<b>0.003</b>	<b>&lt; 0.001</b>	<b>&lt; 0.001</b>	<b>&lt; 0.001</b>	<b>&lt; 0.001</b>
Vegetation	<b>&lt; 0.001</b>	<b>0.002</b>	<b>&lt; 0.001</b>	<b>0.001</b>	<b>&lt; 0.001</b>	<b>&lt; 0.001</b>
Temperature	<b>0.013</b>	<b>0.004</b>	<b>0.004</b>	NS	<b>&lt; 0.001</b>	0.09
Region × elevation	NS	<b>0.003</b>	<b>0.004</b>	<b>&lt; 0.001</b>	0.08	<b>&lt; 0.001</b>
Region × vegetation	<b>0.002</b>	NS	NS	NS	NS	<b>0.002</b>
Elevation × vegetation	<b>0.005</b>	<b>0.005</b>	0.06	NS	0.09	NS

NS: non-significant.

metabolic quotient (*q*CO<sub>2</sub>) relating respiratory activity to microbial biomass in the 12th week of the experiment decreased significantly with decreasing C : N and C : P ratios of the litter layer (Fig. 5) and thus from tundra towards forest (*p*<sub>elevation</sub> < 0.001). It was smallest in the litter layer under tree canopy (*p*<sub>vegetation</sub> < 0.001).

Extracellular enzyme activity was generally higher in the litter layer of the S Urals than in Khibiny (Fig. S4 in the Supplement). Activities of enzyme hydrolyzing organic N (aminidase and peptidase) did not differ among elevation levels and between vegetation types for both mountain regions (Table 4). In comparison, phosphatase activity was higher in the P-poor litter layer of the open vegetation areas than in the P-rich litter layer under tree canopy in the S Urals but showed no consistent pattern with elevation and among vegetation types in Khibiny (*p*<sub>region×vegetation</sub> < 0.001; Fig. S4 in the Supplement). Accordingly, the ratios of the activity of C : P acquiring enzymes of the litter layer correlated nega-

tively with the C : P ratio of the litter layer in the S Urals (*R*<sup>2</sup> = 0.44\*\*) but not in Khibiny (Fig. 5). Ratios of the activity of C : N acquiring enzymes did not correlate with either C : N ratios of the litter layer nor with those of microbial biomass (Fig. 5).

### 3.4 Temperature effects

Carbon mineralization was significantly higher at 15 °C than at 5 °C (Fig. 2; *p*<sub>Temperature</sub> < 0.001) with a *Q*<sub>10</sub> value of 3.3 ± 0.02 (Fig. 6). Also, the release of DOC and DON was significantly increased by warmer temperatures (*p*<sub>Temperature</sub> < 0.001; Table 2), though their average *Q*<sub>10</sub> value was only 1.7 ± 0.02. Temperature effects on net N mineralization varied depending on litter type. In tundra type litter (open areas in the tundra and at treeline) with low net N mineralization rates, temperature had no effects. In forest litter, higher temperatures increased net N mineralization

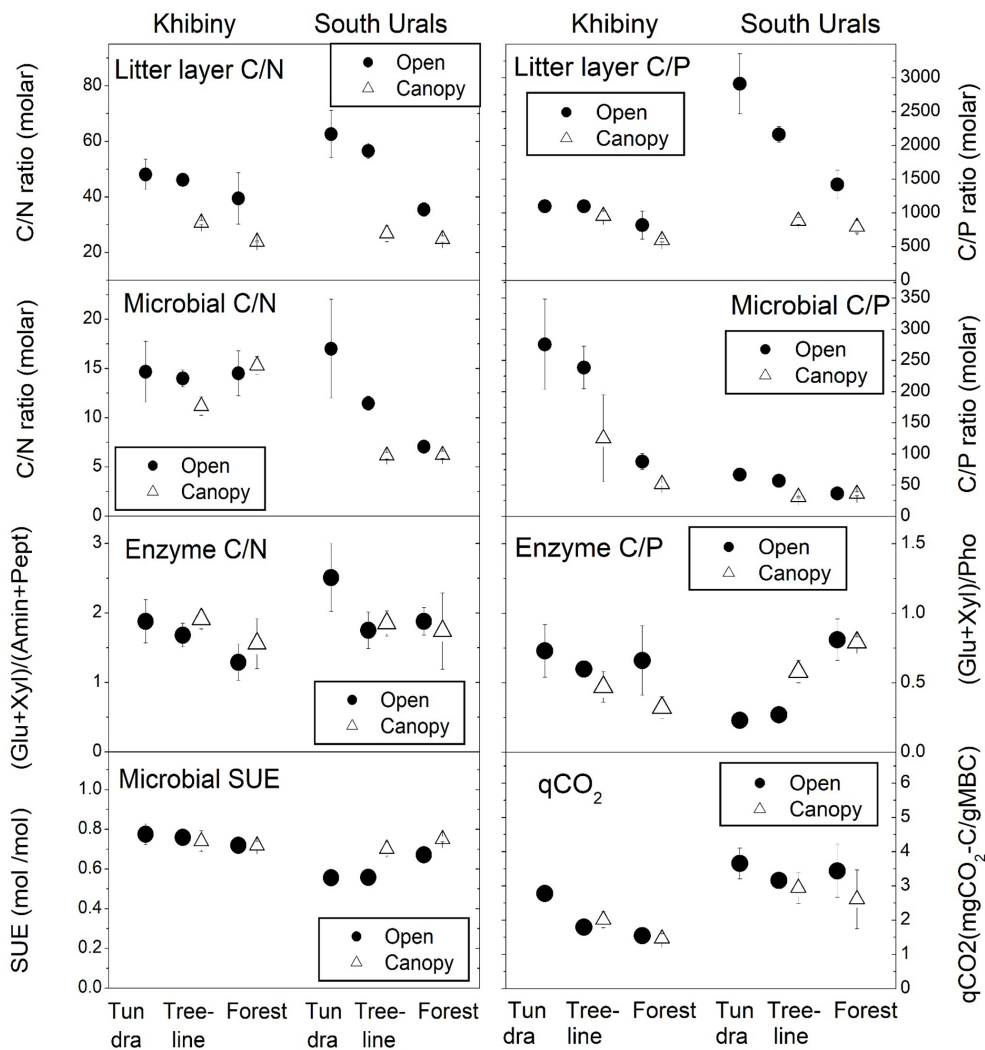


**Figure 5.** Molar C : N and C : P ratios in the litter layer and in microbial biomass, potential activity of element acquiring extracellular enzymes, metabolic quotient ( $q\text{CO}_2$ ), and substrate-use efficiency (SUE) across the forest–tundra ecotones in Khibiny and South Ural mountains. Tundra, treeline, and forest span distinct elevation gradients. Means and standard errors of three plots after a 12-week-long incubation at 15 °C.

**Table 4.** Statistical significance ( $p$  values) of the linear mixed-effects model (LME) testing the effects of region, elevation, vegetation, incubation temperature, and their two-way interactions on extracellular enzyme activity. Data are shown in Fig. S5. Numbers in bold stand for statistically significant results ( $p < 0.05$ ).

	Glucosidase	Xylosidase	Aminidase	Peptidase	Phosphatase
Region	< 0.001	NS	< 0.001	NS	< 0.001
Elevation	0.024	NS	NS	NS	0.01
Vegetation	0.06	NS	NS	NS	NS
Region × elevation	NS	NS	NS	NS	< 0.001
Region × vegetation	NS	NS	NS	NS	0.004
Elevation × vegetation	NS	NS	NS	0.06	NS

NS: non-significant.

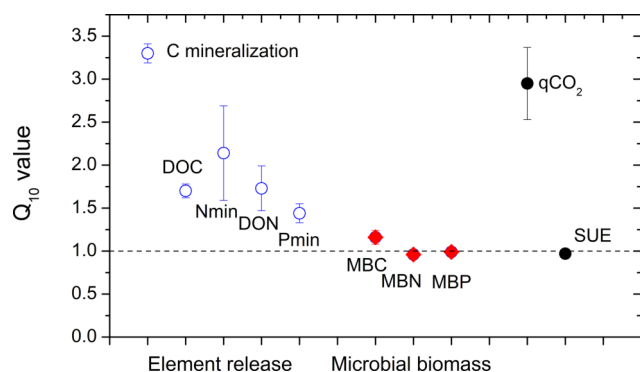


**Figure 6.** Temperature dependencies ( $Q_{10}$  values) of the potential net mineralization of C, N, and P; the release of dissolved organic C and N (DOC and DON); C, N, and P in microbial biomass (MB); metabolic quotient ( $qCO_2$ ); and substrate-use efficiency (SUE) in the litter layer incubated at 5 and 15 °C. Averages and standard errors of all litter layer types in both mountain regions ( $n = 30$ ).

( $p_{\text{Temperature}} = 0.024$ ), resulting in a  $Q_{10}$  value of  $2.0 \pm 0.60$  (Fig. 6). Net P mineralization was not significantly affected by temperature. In forest litter with comparatively high mineralization rates,  $Q_{10}$  values were  $1.34 \pm 0.15$  (Fig. 6). Microbial biomass and their N and P contents were rather independent from temperature (Fig. 6).

### 3.5 Tracking $^{13}\text{C}$ labelled glucose-6-phosphate and substrate-use efficiency (SUE)

The addition of  $^{13}\text{C}$  labelled glucose-6-phosphate (G6P) led to an immediate  $^{13}\text{C}$  enrichment of respired  $\text{CO}_2$  from the litter layer (Fig. S5 in the Supplement). During the following 7 d, between 23 % (litter under conifer trees from the S Urals) and 47 % (tundra litter layer) of the added G6P were mineralized (Fig. 7). Substrate-use efficiency (SUE) increased from the tundra towards forest in the S Urals but not in Khibiny ( $p_{\text{region} \times \text{elevation}} < 0.002$ ; Fig. 5). Overall, SUE was significantly related to litter stoichiometry, correlating more closely with C : P than with the C : N ratios of the litter layer (Fig. S7 in the Supplement). Temperature did not affect SUE (Fig. 6).

The G6P addition did not lead to a net release of dissolved inorganic P (DIP) from G6P in the tundra litter layer with high C : P ratios (Fig. 7) although the amount of P added (0.175 mg P per sample) was more than twice as high as the highest observed P leaching rates from litter material (Fig. S6 in the Supplement). In contrast, in the forest canopy litter with low C : P ratios, G6P addition increased the net DIP release from the litter layer (Fig. 7). However, also here, the G6P-induced increase in net DIP release amounted to maximally 13 % of added P. When relating the net DIP release to the amount of G6P mineralized estimated by the  $^{13}\text{C}$  tracing (22 to 47 % of the added  $^{13}\text{C}$ ), then the net DIP release corresponded to maximally 50 % of P potentially released from mineralized G6P (Fig. 7). In tundra, net DIP release re-

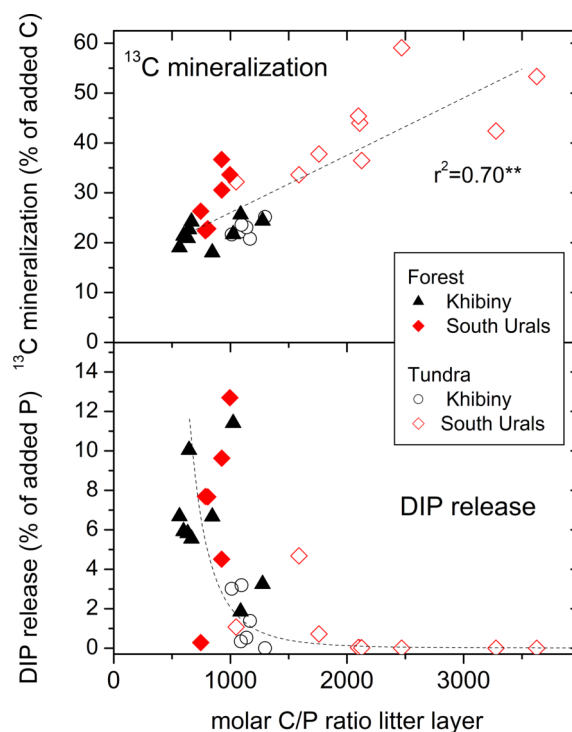


**Figure 7.** Relationship between the molar C : P ratio in the litter layer and the mineralization of  $^{13}\text{C}$  from added  $^{13}\text{C}$  labelled glucose-6-phosphate (G6P) and the net release of dissolved inorganic P (DIP) following the G6P addition in the tundra and forest of the Khibiny Mountains and the South Urals. DIP release is fitted to a threshold-type function ( $y = x/1000^5$ ;  $r^2 = 0.38^{**}$ ).

mained below 10 % of mineralized G6P. Consequently, the greatest fraction of added G6P had been immobilized.

### 3.6 Discussion

#### 3.7 Carbon, nitrogen, and phosphorus release across forest–tundra ecotones

Our study demonstrates that treeline ecotones represent a distinct boundary in litter quality and the C, N, and P release from decomposing litter layer with consequences for ecosystem N and P cycling across treelines. Consistent with our hypothesis, the composition of organic constituents in the litter layer changed, and C : N : P ratios strongly decreased with the shift in plant life forms and species from tundra to forest (Table 1). One reason for the pronounced change in litter stoichiometry is the species-specific stoichiometric homeostasis of plant tissues (Elser et al., 2010). For instance, lichens and mosses in the tundra typically have lower nutrient concentrations compared to the vascular plants in forests (Asplund and Wardle, 2013). Plant–soil feedbacks may reinforce the stoichiometric differences between tundra and forest vegetation, as the smaller C : N : P ratios in forest litter contribute to higher nutrient content in soil organic matter, thereby in-

creasing soil nutrient availability (Fetzer et al., 2024). Additionally, tree roots and associated mycorrhizae can enhance weathering and nutrient mining. While these processes primarily affect P rather than N, enhanced P availability – coupled with molybdenum mobilized in the rhizosphere – can promote  $N_2$  fixation, which is a critical mechanism for N accumulation in Arctic ecosystems (Rousk et al., 2017).

Our results reveal that the changes in stoichiometry in the litter layer across treeline significantly influence the processing of C, N, and P by microbial communities. Most strikingly, potential net N and P mineralization of the litter layer shifted from negligible rates in the treeless tundra to a pronounced nutrient mineralization in the litter layer under tree canopies at lower elevations. In contrast, C mineralization of the litter layer was surprisingly similar across the tree-line ecotone, differing on average only by 16 % between the litter layer in the tundra as compared to the forest (Fig. 2). These small changes are consistent with the litterbag study at treeline by Chen et al. (2018), observing that litter mass loss was less strongly affected by litter quality than by microclimate, which was more favourable below than above tree-line. In our study, we attribute the relatively small changes in C mineralization to the cancelling out of quality characteristics of the litter layer across the forest–tundra ecotone. The forest litter layer had higher lignin contents, generally associated with slower mineralization (Berg and McClaugherty, 2020). However, FT-IR analysis indicated that the forest litter was less aliphatic than tundra litter, a characteristic typically linked to a more rapid mineralization. In contrast to studies with tree litter (Hagedorn and Machwitz, 2007; Cornwell et al., 2008; Moore et al., 2011), C mineralization exhibited a positive correlation with C : N and C : P ratios. This could indicate that in the tundra with high litter C : N : P ratios microorganisms mineralized C in excess to acquire nutrients, a mechanism that has been named as “overflow respiration” (Mooshammer et al., 2014). However, we rather relate the apparent positive relationship between C : N : P ratios and C mineralization to a changing composition in organic constituents along the same trajectory. For instance, while the litter layer under tree canopies had the lowest C : N : P ratio, it also contained the highest contents of lignin, which is more resistant to decomposition.

Despite the rather subtle changes in C mineralization across the forest–tundra ecotone, potential net N and P mineralization showed a threshold type increase from tundra to the forest canopy (Fig. 4). The increased release of mineral N and P by more than a magnitude clearly exceeded a simple “concentration or dilution effect” due to the litter layer having 2 to 5 times smaller N and P concentrations in the tundra than under the forest canopy. Consequently, N and P immobilization must have been contributing to the negligible net nutrient release from the litter layer in the tundra. This conclusion is supported by the experiment tracking the fate of glucose-6-phosphate (G6P). While 20 %–50 % of the  $^{13}C$ -labeled G6P was mineralized within 3 d in the litter layer,

only a small fraction of the added P was released as phosphate (Fig. 7). Again, there was complete net retention of the added P from the easily mineralizable G6P in tundra litter, albeit to a lesser extent in tree canopy litter. Our findings could have been influenced by sorption of mineralized phosphate (Brödlín et al., 2019); however, this seems improbable in the purely organic litter layer, where negatively charged organic matter does not sorb negatively charged  $PO_4^{3-}$ . Thus, phosphate mineralized either from the litter layer itself or from the added G6P must have been immobilized, potentially within microbial biomass, as observed in organic layers with low P availability (Siegenthaler et al., 2024).

In our incubation experiment, the threshold element ratios (TERs), at which net mineralization abruptly switches (Zechmeister-Boltenstern et al., 2015), were about 35 for C : N and 1000 for C : P for the litter layer of the two forest–tundra ecotones (Fig. 4). These TERs correspond to the critical ratios observed in mineralization studies of forest litter layer (e.g. Heuck and Spohn, 2016; Brödlín et al., 2019). For the C : N ratio, the observed TER is also in line with the one estimated from microbial nitrogen use efficiencies of microbial communities (Mooshammer et al., 2014). In our study, the TER for the net DIP release from added G6P (Fig. 7) coincided with the one of net P mineralization again supporting that microbial immobilization causes the negligible DIP release (Fig. 7). The TER observed here, however, is slightly smaller than critical element ratios of net N and P loss estimated by litter bag studies (e.g. Moore et al., 2011; Manzoni et al., 2012). One obvious reason could be that in litterbag studies the export of nutrients through soil fauna and the leaching of nutrients in organic forms is not considered. In our experiment with repeated leaching of litter layer material, the contribution of DON to total N release was particularly high for the low N litter layer in the tundra (60 % on average). Consequently, N leaching losses occurred already above the TER for net N mineralization. We do not expect that DON released from the decomposing tundra litter improves the bioavailability of N in the tundra substantially, as only a small fraction of DON consists of low-molecular-weight compounds such as proteins or amino acids that can be taken up by tundra plants (Weintraub and Schimel, 2005). Moreover, only a small fraction (15 % to 40 %) of dissolved organic matter leached from litter and forest floor layer is biodegradable (Hagedorn and Machwitz, 2007). Even when DON becomes mineralized, released inorganic N will become immobilized in the litter layer with very high C : N ratios, as was the case for phosphate released from mineralized G6P.

### 3.8 Flexible C : P ratios of microbial biomass

Microbial communities are generally regarded as homeostatic (Zechmeister-Boltenstern et al., 2015). In our study, however, C : N : P ratios of microbial biomass increased significantly from the forest towards the nutrient-poorer tun-

dra along with increasing C : N : P ratios in the litter layer (Fig. 5). This lends support for a stoichiometric plasticity of microbial biomass to overcome stoichiometric imbalance between resource material and decomposing communities (Fanin et al., 2017). The increase in microbial stoichiometry was more pronounced in the S Urals than in the Khibiny Mountains, and it was stronger for microbial C : P (molar ratio of 25 to 250) than for microbial biomass C : N (molar ratio of 6 to 15). One reason for the greater plasticity of microbial biomass P could be the greater range in molar C : P ratios (600 to 2900) than in molar C : N ratios (24 to 63) in the litter layer (Fig. 5), possibly stemming from a greater plasticity of plants for P (Yuan and Chen, 2009). Another contributing factor could be shifts in microbial community structure across the forest–tundra ecotone driven by the changes in the composition and origin of the litter layer (Solly et al., 2017a). For instance, the fungi-to-bacteria ratio in the litter layer decreased from tundra to forest in the S Urals (Ika Djukic, unpublished data). Soil fungi exhibit higher C : N : P ratios than bacteria (Mouginot et al., 2014) and fungal guilds show a 2-fold greater range in their C : P ratios than in their C : N ratios (Zhang and Elser, 2017). Thus, microbial community shifts across the forest–tundra ecotone likely play a significant role in the observed plasticity of microbial C : N : P ratios. Also, saprobic fungi were found to possess a more flexible stoichiometry in response to nutrient resources than previously thought (Camenzind et al., 2021). Fungi also show more plasticity in C : P than in C : N ratios, possibly related to the modulating storage of polyphosphates. In our study, the N : P ratio in microbial biomass was rather homeostatic compared to its C : P ratio, likely due to the tight coupling of the synthesis of N-rich proteins with P-demanding ribosomal activity (Loladze and Elser, 2011).

### 3.9 Microbial ecophysiology

Despite the plasticity of the C : N and C : P ratios in microbial biomass, there was still a stoichiometric imbalance between resource material and decomposing communities. Microbial ecophysiology responded in various mechanisms to cope with this imbalance, but their relative importance differed between N and P and the two mountain regions. Consistent with the concept of TER, which assumes that the C flow is controlled by the limiting element (Zechmeister-Boltenstern et al., 2015), the amount of respired CO<sub>2</sub> as compared to microbial biomass ( $q\text{CO}_2$ ) decreased with decreasing C : nutrient ratios and hence from tundra to forest. In agreement, the mineralization of <sup>13</sup>C-labelled G6P increased with increasing C : P and C : N ratios in the litter layer (Fig. 7). However, the <sup>13</sup>C incorporation into microbial biomass remained unaffected by stoichiometry and did not change along the elevation gradient. Therefore, the SUE decreased with increasing C : P and C : N ratios, indicating a smaller production of new microbial biomass per unit C when N and P are scarce (Manzoni et al., 2021), as in tun-

dra litter. Although the release of extracellular enzyme represents one of the mechanisms of microorganisms to overcome nutrient limitation (Manzoni et al., 2021), the only positive correlation of enzymatic activity with C : nutrient ratios of the litter layer existed for phosphatase activity in the S Urals (Fig. 5). The lacking relation of phosphatase activity with litter C : P ratios in Khibiny might be attributed to generally higher P contents and thus C : P ratios below TER, as well as to the pronounced changes of microbial C : P ratios across the forest–tundra ecotone in this region. Consequently, there was no need for microorganisms to invest in the production of phosphatases. In addition, the production of phosphatases might have been limited by the low nitrogen availability, especially in tundra litter layer. Relations of enzyme activities from the N cycle with litter stoichiometry are less straightforward, as organic N molecules also represent an important C source. Therefore their mineralization also depends on C-substrate preferences and/or C limitation of the microbial community (Zechmeister-Boltenstern et al., 2015).

### 3.10 Small temperature effects

While temperature expectedly stimulated C mineralization, the effects of 10 °C warmer temperatures on net dissolved organic and inorganic N and P release were not significant. This may be because microbially driven processes of production and immobilization – which are both temperature sensitive – balanced each other out (Müller et al., 2009). The absence of a temperature response of SUE aligns with findings of Frey et al. (2013) suggesting that temperature enhances both catabolic and anabolic microbial activity to a similar extent. The smaller effect sizes of the +10 °C warmer temperatures compared to litter type on net N and P mineralization imply that indirect effects of climatic warming through changes in plant community composition – for instance by treeline advances – are more influential on soil N and P cycling in the litter layer than direct temperature effects.

### 3.11 Differences between treeline ecotones

Despite the regional differences in bedrock types and tree species, there was a consistent increase in net N and P mineralization from tundra to forest in both regions. However, changes in net C, N, and P mineralization and microbial ecophysiology across the forest–tundra ecotone were more pronounced in the S Urals than in the Khibiny Mountains. One likely reason is the dominance of different tree species, while broadleaf trees dominate in the Khibiny Mountains, and coniferous trees form the high-elevation forest in the S Urals. This created a more pronounced contrast in the quality of the litter layer from tundra to forest in the S Urals, whereas both deciduous shrubs and trees in Khibiny produce annual leaves above and below the treeline. Another factor could be the P-rich plutonic bedrock in the Khibiny Mountains, compared to the quartzitic bedrock in the S Urals. Con-

sequently, the gradient in the C : P ratios of the litter layer from the forest to the tundra was less pronounced in Khibiny than in the S Urals. However, further studies are needed to better understand the modulating influence of soil fertility and plants species composition on C and nutrient dynamics at treeline.

### 3.12 Ecosystem-scale processes

Our study supports the concept of a positive litter feedback at treeline, which likely contributes to the distinct increase in nutrient availability from tundra to forest ecosystems (Fetzer et al., 2024). Forest plants, including trees and understory species, growing in soils with a higher N and P availability than tundra (Table S2 in the Supplement), produce nutrient-rich litter. This in turn releases greater amounts of inorganic nutrients during decomposition, further enhancing N and P availability. The litter feedback may influence plant growth, reducing vigour in the tundra while promoting it in the forest – a conclusion supported by fertilization experiments at treeline in the Scandes and in the Alps, where significant growth responses were observed even at low fertilizer doses (Sveinbjörnsson, 2000; Sullivan et al., 2015; Möhl et al., 2018). Similarly, an analogous feedback driving enhanced shrub growth has been proposed for Arctic regions (e.g. Buckeridge et al., 2010).

We are aware that our laboratory experiment estimated only potential net N and P mineralization, while in situ rates can additionally be influenced by moisture patterns, freeze-thaw cycles (Gao et al., 2020, 2021), soil biota, or plant-mediated processes (Fetzer et al., 2024). Furthermore, N and P immobilized in microbial biomass and incorporated into soil organic matter become eventually released during mineralization of microbial necromass and/or SOM with lower C-to-nutrient ratios (see, for N, Knops et al., 2002). However, regardless of whether N and P are released directly from the litter or following microbial recycling, the nutrient release per unit litter produced is much greater in the forest than in tundra. This is supported by higher contents of available N and P in the soil beneath the litter layer in the forest compared to the tundra (Table S2). Also, other treeline ecotones in various temperate regions around the globe show increasing available N and P contents in the soil from tundra towards forest (Mayor et al., 2017).

## 4 Conclusions

Our study highlights treeline ecosystems as a distinct boundary in the C, N, and P release from decomposing litter layer with consequences for ecosystem N and P cycling across treeline. Due to substantial changes in litter stoichiometry from tundra to forest, net N and P mineralization from the litter layer was negligible in the tundra due to microbial immobilization in the nutrient-poor litter, while large amounts

of N and P were mineralized in the forest. Microbial eco-physiology paralleled these changes, including more efficient use of organic matter by microorganisms in the forest where litter C : N : P ratios were lower than in tundra. Additionally, microbial biomass C : nutrient ratios decreased from tundra to forest with greater plasticity observed for microbial C : P than C : N ratios. The production of extracellular enzymes appeared less sensitive. Results also showed that the 10 °C temperature gradient had less impact on net N and P mineralization than litter stoichiometry, suggesting that indirect effects of climatic effects such as plant species shifts are more important for N and P cycling than direct temperature effects. We propose that the pronounced shift in net N and P mineralization across treelines triggers a positive “litter feedback”, where forest expansion driven by warming will reduce C-to-nutrient ratios in decomposing organic matter compared to tundra. This will in turn accelerate nutrient cycling and enhance nutrient availability, potentially promoting the productivity of the advancing forest.

*Data availability.* All data are openly available at <https://doi.org/10.16904/envdatat.536> (Hagedorn, 2024).

*Supplement.* The supplement related to this article is available online at <https://doi.org/10.5194/bg-22-2959-2025-supplement>.

*Author contributions.* PM and FH established the sampling design in the field. FH and JF sampled the litter layer. EF contributed to the conception of the study. FH, JF, JI, DC, PS, and DG designed and performed the laboratory study and analysis. JF, JI, and FH conducted the data analyses and the data visualization and wrote the first draft of the paper. All authors contributed to the interpretation of the findings and to the revision of the paper, and they read and approved the submitted version.

*Competing interests.* At least one of the (co-)authors is a member of the editorial board of *Biogeosciences*. The peer-review process was guided by an independent editor, and the authors also have no other competing interests to declare.

*Disclaimer.* Publisher’s note: Copernicus Publications remains neutral with regard to jurisdictional claims made in the text, published maps, institutional affiliations, or any other geographical representation in this paper. While Copernicus Publications makes every effort to include appropriate place names, the final responsibility lies with the authors.

*Special issue statement.* This article is part of the special issue “Treeline ecotones under global change: linking spatial patterns to ecological processes”. It is not associated with a conference.



**Acknowledgements.** We gratefully acknowledge the financial support for Jasmin Fetzer and Frank Hagedorn by the Swiss National Science Foundation (SNF) (project number 171171). We thank the WSL central laboratory (Alessandro Schlumpf, Karin von Känel, Janka Bollenbach, Ursula Graf, Daniele Pezzotta), the WSL forest soil laboratory (Alois Zürcher, Behzad Rahimi, Nouredine Hajjar), and field teams for their support. We are also grateful to Philipp Baumann (ETH Zurich) for his support in measuring FT-IR spectra and Andri Baltensweiler for creating the map. This work was performed within the framework of the joint projects conceived by the Institute of Plant and Animal Ecology of the Ural Branch of the Russian Academy of Science (IPAE) and the Swiss Federal Institute for Forest, Snow, and Landscape Research (WSL).

**Financial support.** This research has been supported by the Swiss National Science Foundation (SNF) (grant no. 171171).

**Review statement.** This paper was edited by Matteo Garbarino and reviewed by two anonymous referees.

## References

- Adamczyk, B., Sietiö, O. M., Straková, P., Prommer, J., Wild, B., Hagner, M., Pihlatie, M., Fritze, H., Richter, A., and Heinonsalo, J.: Plant roots increase both decomposition and stable organic matter formation in boreal forest soil, *Nat. Commun.*, 10, 3982, <https://doi.org/10.1038/s41467-019-11993-1>, 2019.
- Aerts, R.: Climate, leaf litter chemistry and leaf litter decomposition in terrestrial ecosystems: a triangular relationship, *Oikos*, 79, 439–449, <https://doi.org/10.2307/3546886>, 1997.
- Asplund, J. and Wardle, D. A.: The impact of secondary compounds and functional characteristics on lichen palatability and decomposition, *J. Ecol.*, 101, 689–700, <https://doi.org/10.1111/1365-2745.12075>, 2013.
- Berg, B. and McClaugherty, C.: Decomposition as a process—some main features in plant litter: decomposition, humus formation, carbon sequestration, Springer International Publishing, Cham, [https://doi.org/10.1007/978-3-030-59631-6\\_2](https://doi.org/10.1007/978-3-030-59631-6_2), 13–43, 2020.
- Brödl, D., Kaiser, K., and Hagedorn, F.: Divergent patterns of carbon, nitrogen, and phosphorus mobilization in forest soils, *Front. For. Glob. Chang.*, 2, 66, <https://doi.org/10.3389/ffgc.2019.00066>, 2019.
- Brookes, P. C., Powlson, D. S., and Jenkinson, D. S.: Measurement of microbial biomass phosphorus in rhizosphere soil, *Soil Biol. Biochem.*, 14, 319–329, [https://doi.org/10.1016/0038-0717\(82\)90001-3](https://doi.org/10.1016/0038-0717(82)90001-3), 1982.
- Brookes, P. C., Landman, A., Pruden, G., and Jenkinson, D. S.: Chloroform fumigation and the release of soil nitrogen: A rapid direct extraction method to measure microbial biomass nitrogen in soil, *Soil Biol. Biochem.*, 17, 837–842, [https://doi.org/10.1016/0038-0717\(85\)90144-0](https://doi.org/10.1016/0038-0717(85)90144-0), 1985.
- Buckeridge, K. M., Zufelt, E., Chu, H., and Grogan, P.: Soil nitrogen cycling rates in low arctic shrub tundra are enhanced by litter feedbacks, *Plant Soil*, 330, 407–421, <https://doi.org/10.1007/s11104-009-0214-8>, 2010.
- Büntgen, U., Piermattei, A., Crivellaro, A., Reinig, F., Krušic, P. J., Trnka, M., Torbenson, M., Esper, J.: Common Era treeline fluctuations and their implications for climate reconstructions, *Global Planet. Change*, 219, 103979, <https://doi.org/10.1016/j.gloplacha.2022.103979>, 2022.
- Camenzind, T., Philipp Grenz, K., Lehmann, J., and Rillig, M. C.: Soil fungal mycelia have unexpectedly flexible stoichiometric C : N and C : P ratios, *Ecol. Lett.*, 24, 208–218, <https://doi.org/10.1111/ele.13632>, 2021.
- Canali, S. and Benedetti, A.: Soil nitrogen mineralization, in: *Microbiological Methods for Assessing Soil Quality*, edited by: Bloem, J., Hopkins, D. W., and Benedetti, A., CABI, Wallingford, UK, 23–49, ISBN: 978-1-84593-500-9, 2006.
- Chen, Y., Liu, Y., Zhang, J., Yang, W., He, R., and Den, C.: Microclimate exerts greater control over litter decomposition and enzyme activity than litter quality in an alpine forest-tundra ecotone, *Sci. Rep.-UK*, 8, 14998, <https://doi.org/10.1038/s41598-018-33186-4>, 2018.
- Cornwell, W. K., Cornelissen, J. H. C., Amatangelo, K., Dorrepaal, E., Eviner, V. T., Godoy, O., Hobbie, S. E., Hoorens, B., Kurokawa, H., Pérez-Harguindeguy, N., Quested, H. M., Santiago, L. S., Wardle, D. A., Wright, I. J., Aerts, R., Allison, S. D., Van Bodegom, P., Brovkin, V., Chatain, A., Callaghan, T. V., Díaz, S., Garnier, E., Gurvich, D. E., Kazakou, E., Klein, J. A., Read, J., Reich, P. B., Soudzilovskaia, N. A., Vaieretti, M. V., and Westoby, M.: Plant species traits are the predominant control on litter decomposition rates within biomes worldwide, *Ecol. Lett.*, 11, 1065–1071, <https://doi.org/10.1111/j.1461-0248.2008.01219.x>, 2008.
- Duboc, O., Zehetner, F., Djukic, I., Tatzber, M., Berger, T. W., and Gerzabek, M. H.: Decomposition of European beech and Black pine foliar litter along an Alpine elevation gradient: Mass loss and molecular characteristics, *Geoderma*, 189–190, 522–531, <https://doi.org/10.1016/j.geoderma.2012.06.018>, 2012.
- Elser, J. J., Fagan, W. F., Kerkhoff, A. J., Swenson, N. G., and Enquist, B. J.: Biological stoichiometry of plant production: metabolism, scaling and ecological response to global change, *New Phytol.*, 186, 593–608, <https://doi.org/10.1111/j.1469-8137.2010.03214.x>, 2010.
- Fanin, N., Fromin, N., Barantal, S., and Hättenschwiler, S.: Stoichiometric plasticity of microbial communities is similar between litter and soil in a tropical rainforest, *Sci. Rep.-UK*, 7, 1–7, <https://doi.org/10.1038/s41598-017-12609-8>, 2017.
- Fetzer, J., Frossard, E., Kaiser, K., and Hagedorn, F.: Leaching of inorganic and organic phosphorus and nitrogen in contrasting beech forest soils – seasonal patterns and effects of fertilization, *Biogeosciences*, 19, 1527–1546, <https://doi.org/10.5194/bg-19-1527-2022>, 2022.
- Fetzer, J., Moiseev, P., Frossard, E., Kaiser, K., Mayer, M., Gavazov, K., and Hagedorn, F.: Plant-soil interactions drive nitrogen and phosphorus dynamics in an advancing subarctic treeline, *Glob. Change Biol.*, 30, e17200, <https://doi.org/10.1111/gcb.17200>, 2024.
- Frey, S. D., Lee, J., Melillo, J. M., and Six, J.: The temperature response of soil microbial efficiency and its feedback to climate, *Nat. Clim. Change*, 3, 395–398, <https://doi.org/10.1038/nclimate1796>, 2013.
- Gao, D., Bai, E., Li, M., Zhao, C., Yu, K., and Hagedorn, F.: Responses of soil nitrogen and phosphorus cycling to drying and

- rewetting cycles: A meta-analysis, *Soil Biol. Biochem.*, 148, 107896, <https://doi.org/10.1016/j.soilbio.2020.107896>, 2020.
- Gao, D., Bai, E., Yang, Y., Zong, S., and Hagedorn, F.: A global meta-analysis on freeze-thaw effects on soil carbon and phosphorus cycling, *Soil Biol. Biochem.*, 159, 108283, <https://doi.org/10.1016/j.soilbio.2021.108283>, 2021.
- Gavazov, K. S.: Dynamics of alpine plant litter decomposition in a changing climate, *Plant Soil*, 337, 19–32, <https://doi.org/10.1007/s1104-010-0477-0>, 2010.
- German, D. P., Weintraub, M. N., Grandy, A. S., Lauber, C. L., Rinkes, Z. L., and Allison, S. D.: Optimization of hydrolytic and oxidative enzyme methods for ecosystem studies, *Soil Biol. Biochem.*, 43, 1387–1397, <https://doi.org/10.1016/j.soilbio.2011.03.017>, 2011.
- Gustafson, A., Miller, P. A., Björk, R. G., Olin, S., and Smith, B.: Nitrogen restricts future sub-arctic treeline advance in an individual-based dynamic vegetation model, *Biogeosciences*, 18, 6329–6347, <https://doi.org/10.5194/bg-18-6329-2021>, 2021.
- Hagedorn, F.: C-N-P-Release Treeline, *EnviDat* [data set], <https://doi.org/10.16904/envidat.536>, 2024.
- Hagedorn, F. and Machwitz, M.: Controls on dissolved organic matter leaching from forest litter grown under elevated atmospheric CO<sub>2</sub>, *Soil Biol. Biochem.*, 39, 1759–1769, <https://doi.org/10.1016/j.soilbio.2007.01.038>, 2007.
- Hagedorn, F., Shiyatov, S. G., Mazepa, V. S., Devi, N. M., Grigor'ev, A. A., Bartysh, A. A., Fomin, V. V., Kapralov, D. S., Terent'ev, M., Bugman, H., and Rigling, A.: Tree-line advances along the Urals mountain range–driven by improved winter conditions? *Glob. Change Biol.*, 20, 3530–3543, <https://doi.org/10.1111/gcb.12613>, 2014.
- Hagedorn, F., Gavazov, K., and Alexander, J. M.: Above- and belowground linkages shape responses of mountain vegetation to climate change, *Science*, 365, 1119–1123, <https://doi.org/10.1126/science.aax4737>, 2019.
- Hagedorn, F., Dawes, M. A., Bubnov, M. O., Devi, N. M., Grigor'ev, A. A., Mazepa, V. S., and Moiseev, P. A.: Latitudinal decline in stand biomass and productivity at the elevational treeline in the Ural mountains despite a common thermal growth limit, *J. Biogeogr.*, 47, 1827–1842, <https://doi.org/10.1111/jbi.13867>, 2020.
- Heuck, C. and Spohn, M.: Carbon, nitrogen and phosphorus net mineralization in organic horizons of temperate forests: stoichiometry and relations to organic matter quality, *Biogeochemistry*, 131, 229–242, <https://doi.org/10.1007/s10533-016-0276-7>, 2016.
- Joly, F. X., Scherer-Lorenzen, M., and Hättenschwiler, S.: Resolving the intricate role of climate in litter decomposition, *Nat. Ecol. Evol.*, 7, 214–223, <https://doi.org/10.1038/s41559-022-01948-z>, 2023.
- Kaiser, C., Franklin, O., Richter, A., and Dieckmann, U.: Social dynamics within decomposer communities lead to nitrogen retention and organic matter build-up in soils, *Nat. Commun.*, 6, 8960, <https://doi.org/10.1038/ncomms9960>, 2015.
- Kammer, A., Hagedorn, F., Shevchenko, I., Leifeld, J., Guggenberger, G., Goryacheva, T., Rigling, A., and Moiseev, P. A.: Treeline shifts in the Ural mountains affect soil organic matter dynamics, *Glob. Change Biol.*, 15, 1570–1583, <https://doi.org/10.1111/j.1365-2486.2009.01856.x>, 2009.
- Knops, J. M. H., Bradley, K. L., and Wedin, D. A.: Mechanisms of plant species impacts on ecosystem nitrogen cycling, *Ecol. Lett.*, 5, 454–466, <https://doi.org/10.1046/j.1461-0248.2002.00332.x>, 2002.
- Körner, C. and Paulsen, J.: A world-wide study of high altitude treeline temperatures, *J. Biogeogr.*, 31, 713–732, <https://doi.org/10.1111/j.1365-2699.2003.01043.x>, 2004.
- Liu, Y., Chen, Y., Zhang, J., Yang, W., Peng, Z., He, X., Deng, C., and He, R.: Changes in foliar litter decomposition of woody plants with elevation across an alpine forest–tundra ecotone in eastern Tibet Plateau, *Plant Ecol.*, 217, 495–504, <https://doi.org/10.1007/s11258-016-0594-9>, 2016.
- Liu, Y., Wang, L., He, R., Chen, Y., Xu, Z., Tan, B., Zhang, L., Xiao, J., Zhu, P., and Chen, L.: Higher soil fauna abundance accelerates litter carbon release across an alpine forest–tundra ecotone, *Sci. Rep.-UK*, 9, 10561, <https://doi.org/10.1038/s41598-019-47072-0>, 2019.
- Loladze, I. and Elser, J. J.: The origins of the Redfield nitrogen-to-phosphorus ratio are in a homeostatic protein-to-rRNA ratio, *Ecol. Lett.*, 14, 244–250, <https://doi.org/10.1111/j.1461-0248.2010.01577.x>, 2011.
- Makarov, M. I., Malysheva, T. I., Menyailo, O. V., Soudzilovskaia, N. A., Van Logtestijn, R. S. P., and Cornelissen, J. H. C.: Effect of K<sub>2</sub>SO<sub>4</sub> concentration on extractability and isotope signature ( $\delta^{13}\text{C}$  and  $\delta^{15}\text{N}$ ) of soil C and N fractions, *Eur. J. Soil Sci.*, 66, 417–426, <https://doi.org/10.1111/ejss.12243>, 2015.
- Manzoni, S., Schimel, J. P., and Porporato, A.: Responses of soil microbial communities to water stress: Results from a meta-analysis, *Ecology*, 93, 930–938, <https://doi.org/10.1890/11-0026.1>, 2012.
- Manzoni, S., Chakrawal, A., Spohn, M., and Lindahl, B. D.: Modeling microbial adaptations to nutrient limitation during litter decomposition, *Front. For. Glob. Chang.*, 4, 1–23, <https://doi.org/10.3389/ffgc.2021.686945>, 2021.
- Mayor, J. R., Sanders, N. J., Classen, A. T., Bardgett, R. D., Clément, J. C., Fajardo, A., Lavorel, S., Sundqvist, M. K., Bahn, M., Chusholm, C., Cieraad, E., Gedalof, Z., Kudo, K. G., Ober-ski, D. L., and Wardle, D. A.: Elevation alters ecosystem properties across temperate treelines globally, *Nature*, 542, 91–95, <https://doi.org/10.1038/nature21027>, 2017.
- Möhl, P., Mörsdorf, M. A., Dawes, M. A., Hagedorn, F., Bebi, P., Viglietti, D., Freppaz, M., Wipf, S., Körner, C., Thomas, F. M., and Rixen, C.: Twelve years of low nutrient input stimulates growth of trees and dwarf shrubs in the treeline ecotone, *J. Ecol.*, 1–13, <https://doi.org/10.1111/1365-2745.13073>, 2018.
- Moiseev, P. A., Hagedorn, F., Balakin, D. S., Bubnov, M. O., Devi, N. M., Kukarskih, V. V., Mazepa, V. S., Viyukhina, S. O., and Grigor'ev, A. A.: Stand biomass at treeline ecotone in Russian Subarctic Mountains is primarily related to species composition but its dynamics driven by improvement of climatic conditions, *Forests*, 13, 254, <https://doi.org/10.3390/f13020254>, 2022.
- Moore, T. R., Trofymow, J. A., Prescott, C. E., and Titus, B. D.: Nature and nurture in the dynamics of C, N and P during litter decomposition in Canadian forests, *Plant Soil*, 339, 163–175, <https://doi.org/10.1007/s1104-010-0563-3>, 2011.
- Mooshammer, M., Wanek, W., Zechmeister-Boltenstern, S., and Richter, A.: Stoichiometric imbalances between terrestrial decomposer communities and their resources: Mechanisms and implications of microbial adaptations to their resources, *Front. Microbiol.*, 5, 1–10, <https://doi.org/10.3389/fmicb.2014.00022>, 2014.

- Mouginot, C., Kawamura, R., Matulich, K. L., Berlemont, R., Allison, S. D., Amend, A. S., and Martiny, A. C.: Elemental stoichiometry of Fungi and Bacteria strains from grassland leaf litter, *Soil Biol. Biochem.*, 76, 278–285, <https://doi.org/10.1016/j.soilbio.2014.05.011>, 2014.
- Müller, M., Alewell, C., and Hagedorn, F.: Effective retention of litter-derived dissolved organic carbon in organic layers, *Soil Biol. Biochem.*, 41, 1066–1074, <https://doi.org/10.1016/j.soilbio.2009.02.007>, 2009.
- Nadelhoffer, K. J., Giblin, A. E., Shaver, G. R., and Laundre, J. A.: Effects of temperature and substrate quality on element mineralization in six arctic soils, *Ecology*, 72, 242–253, <https://doi.org/10.2307/1938918>, 1991.
- Ohno, T. and Zibilske, L. M.: Determination of low concentrations of phosphorus in soil extracts using malachite green, *Soil Sci. Soc. Am. J.*, 55, 892–895, <https://doi.org/10.2136/sssaj1991.03615995005500030046x>, 1991.
- Parker, T. C., Sanderman, J., Holden, R. D., Blume-Werry, G., Sjögersten, S., Large, D., Castro-Diaz, M., Street, L. E., Subke, J. A., and Wookey, P. A.: Exploring drivers of litter decomposition in a greening Arctic: results from a transplant experiment across a treeline, *Ecology*, 99, 2284–2294, <https://doi.org/10.1002/ecy.2442>, 2018.
- Pinheiro, J., Bates, D., DebRoy, S., Sarkar, D., and R Core Team: nlme: Linear and Nonlinear Mixed Effects Models, <https://cran.r-project.org/package=nlme> (last access: 5 July 2024), 2021.
- R Core Team: R: A language and environment for statistical computing, <https://www.r-project.org/> (last access: 27 November 2024), 2020.
- Rousk, K., Degboe, J., Michelsen, A., Bradley, R., and Bellenger, J.-P.: Molybdenum and phosphorus limitation of moss-associated nitrogen fixation in boreal ecosystems, *New Phytol.*, 214, 97–107, <https://doi.org/10.1111/nph.14331>, 2017.
- Sainte-Marie, J., Barrandon, M., Saint-André, L., Gelhaye, E., Martin, F., and Derrien, D.: C-STABILITY an innovative modeling framework to leverage the continuous representation of organic matter, *Nat. Commun.*, 12, 1–13, <https://doi.org/10.1038/s41467-021-21079-6>, 2021.
- Saiya-Cork, K. R., Sinsabaugh, R. L., and Zak, D. R.: The effects of long term nitrogen deposition on extracellular enzyme activity in an *Acer saccharum* forest soil, *Soil Biol. Biochem.*, 34, 1309–1315, [https://doi.org/10.1016/S0038-0717\(02\)00074-3](https://doi.org/10.1016/S0038-0717(02)00074-3), 2002.
- Siegenthaler, M. B., McLaren TI, Frossard E, and Tamburini, F.: Dual isotopic ( $^{33}\text{P}$  and  $^{18}\text{O}$ ) tracing and solution  $^{31}\text{P}$  NMR spectroscopy to reveal organic phosphorus synthesis in organic soil horizons, *Soil Biol. Biochem.*, 197, 109519, <https://doi.org/10.1016/j.soilbio.2024.109519>, 2024.
- Solly, E. F., Lindahl, B. D., Dawes, M. A., Peter, M., Souza, R. C., Rixen, C., and Hagedorn, F.: Experimental soil warming shifts the fungal community composition at the alpine treeline, *New Phytol.*, 215, 766–778, <https://doi.org/10.1111/nph.14603>, 2017a.
- Solly, E. F., Djukic, I., Moiseev, P. A., Andreyashkina, N. I., Devi, N. M., Göransson, H., Mazepa, V. S., Moiseev, P. A., Shiyatov, S. G., Trubina, M. R., Schweingruber, F. H., Wilmking, M., and Hagedorn, F.: Treeline advances and associated shifts in the ground vegetation alter fine root dynamics and mycelia production in the South and Polar Urals, *Oecologia*, 183, 571–586, <https://doi.org/10.1007/s00442-016-3785-0>, 2017b.
- Spohn, M.: Microbial respiration per unit microbial biomass depends on litter layer carbon-to-nitrogen ratio, *Biogeosciences*, 12, 817–823, <https://doi.org/10.5194/bg-12-817-2015>, 2015.
- Spohn, M. and Berg, B.: Import and release of nutrients during the first five years of plant litter decomposition, *Soil Biol. Biochem.*, 176, 108878, <https://doi.org/10.1016/j.soilbio.2022.108878>, 2023.
- Spohn, M. and Widdig, M.: Turnover of carbon and phosphorus in the microbial biomass depending on phosphorus availability, *Soil Biol. Biochem.*, 113, 53–59, <https://doi.org/10.1016/j.soilbio.2017.05.017>, 2017.
- Sullivan, P. F., Ellison, S. B. Z., McNown, R. W., Brownlee, A. H., and Sveinbjörnsson, B.: Evidence of soil nutrient availability as the proximate constraint on growth of treeline trees in north-west Alaska, *Ecology*, 96, 716–727, <https://doi.org/10.1890/14-0626.1>, 2015.
- Sveinbjörnsson, B.: North American and European treelines: External forces and internal processes controlling position, *Ambio*, 29, 388–395, <https://doi.org/10.1579/0044-7447-29.7.388>, 2000.
- Tatzber, M., Mutsch, F., Mentler, A., Leitgeb, E., Englisch, M., and Gerzabek, M. H.: Determination of organic and inorganic carbon in forest soil samples by mid-infrared spectroscopy and partial least squares regression, *Appl. Spectrosc.*, 64, 1167–1175, <https://doi.org/10.1366/000370210792973460>, 2010.
- Tiessen, H. and Moir, J. O.: Characterization of available P by sequential extraction, in: Soil sampling and methods of analysis, edited by: Carter, M. R. and Gregorich, E. G., Canadian Society of Soil Science, 293–306, Boca Raton, ISBN-10: 0873718615, 1993.
- Vance, E. D., Brookes, P. C., and Jenkinson, D. S.: Microbial biomass measurements in forest soils: The use of the chloroform fumigation-incubation method in strongly acid soils, *Soil Biol. Biochem.*, 19, 697–702, [https://doi.org/10.1016/0038-0717\(87\)90051-4](https://doi.org/10.1016/0038-0717(87)90051-4), 1987.
- Wang, L., Chen, Y., Zhou, Y., Zheng, H., Xu, Z., Tan, B., You C., Zhang L., Li, H., Guo L., Wang L., Huang, Y., Zhang, J., and Liu, Y.: Litter chemical traits strongly drove the carbon fractions loss during decomposition across an alpine treeline ecotone, *Sci. Total Environ.*, 753, 142287, <https://doi.org/10.1016/j.scitotenv.2020.142287>, 2021.
- Weintraub, M. N. and Schimel, J. P.: The seasonal dynamics of amino acids and other nutrients in Alaskan Arctic tundra soils, *Biogeochemistry*, 73, 359–380, <https://doi.org/10.1007/s10533-004-0363-z>, 2005.
- Wu, J., Joergensen, R. G., Pommerening, B., Chaussod, R., and Brookes, P. C.: Measurement of soil microbial biomass C by fumigation-extraction-an automated procedure. *Soil Biol. Biochem.*, 22, 1167–1169, [https://doi.org/10.1016/0038-0717\(90\)90046-3](https://doi.org/10.1016/0038-0717(90)90046-3), 1990.
- Yuan, Z. Y. and Chen, H. Y. H.: Global trends in senesced-leaf nitrogen and phosphorus, *Global Ecol. Biogeogr.*, 18, 532–542, <https://doi.org/10.1111/j.1466-8238.2009.00474.x>, 2009.
- Zechmeister-Boltenstern, S., Keiblinger, K. M., Mooshammer, M., Peñuelas, J., Richter, A., Sardans, J., and Wanek, W.: The application of ecological stoichiometry to plant-microbial-soil organic matter transformations, *Ecol. Monogr.*, 85, 133–155, <https://doi.org/10.1890/14-0777.1>, 2015.

Zhang, J. and Elser, J. J.: Carbon: Nitrogen: Phosphorus stoichiometry in fungi: A meta-analysis, *Front. Microbiol.*, 8, 1–9, <https://doi.org/10.3389/fmicb.2017.01281>, 2017.

Zheng, H., Chen, Y., Liu, Y., Zhang, J., Yang, W., Yang, L., Li, H., Wang, L., Wu, F., and Guo, L.: Litter quality drives the differentiation of microbial communities in the litter horizon across an alpine treeline ecotone in the eastern Tibetan Plateau, *Sci. Rep.-UK*, 8, 1–11, <https://doi.org/10.1038/s41598-018-28150-1>, 2018.